

# Photocatalytic Conversion of Diluted CO<sub>2</sub> into Light Hydrocarbons Using Periodically Modulated Multiwalled Nanotube Arrays\*\*

Xiaojiang Zhang, Fei Han, Bo Shi, Samira Farsinezhad, Greg P. Dechaine, and Karthik Shankar\*

Solar-energy-driven conversion of CO<sub>2</sub> into hydrocarbon fuels can simultaneously generate chemical fuels to meet energy demand and mitigate rising CO<sub>2</sub> levels. The utilization of the clean and renewable solar power resource is, on a long-term basis, an essential component of solutions to address growing global energy demand, which is projected to be 40 TW by 2050.<sup>[1]</sup> This is because the solar energy received on the earth's surface in one hour exceeds current total global energy demand. From the perspective of climate change, expansion of the current fossil fuel-based energy infrastructure to meet the projected energy demand is predicted to add 2986–7402 Gt of CO<sub>2</sub> to the atmosphere by 2100, resulting in a mean rise in global temperature of 2.4–4.5 °C.<sup>[2]</sup>

Since the discovery of the photoreduction of carbon dioxide to form organic compounds using semiconductors by Fujishima and co-workers in 1979,<sup>[3]</sup> a growing interest in the development of catalysts that are capable of solar-based capture and storage of CO<sub>2</sub> has evolved.<sup>[4]</sup> Titanium dioxide, which is a cost-efficient, non-toxic and abundant *n*-type semiconductor, has been widely considered in the solar-driven reduction of CO<sub>2</sub>. Owing to its large band-gap energy of 3–3.2 eV, TiO<sub>2</sub> without doping or post-synthesis treatments can absorb only the ultraviolet portion of the solar spectrum. To narrow the band-gap of TiO<sub>2</sub> and improve its photocatalytic performance, strategies such as compositional doping or deliberately introducing disorder in crystalline TiO<sub>2</sub> are being investigated.<sup>[5]</sup> Herein, we demonstrate an approach that is able to achieve high-rate sunlight-driven conversion of diluted CO<sub>2</sub> to light hydrocarbons in which an optimized combination of a Cu-Pt coating and modulated-diameter TiO<sub>2</sub>

nanotubes are used as the photocatalyst. We demonstrate at least a fourfold improvement in CO<sub>2</sub> conversion rates over prior art<sup>[6]</sup> by using a catalyst consisting of coaxial Cu-Pt bimetallic shells supported on a periodically modulated double-walled TiO<sub>2</sub> nanotube (PMTiNT) array core. The photocatalytic reaction occurs at room temperature and generates CH<sub>4</sub>, C<sub>2</sub>H<sub>4</sub>, and C<sub>2</sub>H<sub>6</sub> as reaction products. Under AM1.5 one-sun illumination, using 99.9 % CO<sub>2</sub>, we obtained a hydrocarbon production rate of 3.51 mL g<sup>-1</sup> h<sup>-1</sup> or 574 nmol cm<sup>-2</sup> h<sup>-1</sup>. A key novelty is the effectiveness of our photocatalyst for the photoreduction of unconcentrated CO<sub>2</sub>. When the Cu<sub>0.33</sub>-Pt<sub>0.67</sub>/PMTiNT heterogeneous catalyst was utilized for the photoreduction of diluted CO<sub>2</sub> (0.998 % in N<sub>2</sub>) at 25 °C, we found an average hydrocarbon production rate of 3.7 mL g<sup>-1</sup> h<sup>-1</sup> or 610 nmol cm<sup>-2</sup> h<sup>-1</sup>. The periodic modulation of the diameters of the nanotube arrays increased the surface area and improved the utilization of light while the bimetallic coating increased catalyst activity and specificity. Our version of a highly active CO<sub>2</sub> reduction system does not require reactant gases with high purities and could potentially be used to photocatalytically capture CO<sub>2</sub> directly from air or from flue gas.

A SEM image (Figure 1 A) shows the top-view of a nanotube array photocatalyst. The average diameters of the outer wall and inner wall are 180 ± 10 nm and 130 ± 10 nm, respectively. High-resolution XPS spectra of the TiO<sub>2</sub>-supported Pt-Cu nanotube catalyst (Figure 1 B,C) and energy-dispersive X-ray spectroscopy (EDX) mapping (Figure 1 D) verify that the surfaces of these catalysts are enriched with both copper and platinum. The Pt-Cu coating exists throughout the length of the nanotubes. The peak of Cu2p<sub>3/2</sub> is at 931.2 eV, whereas the peak of Pt4f<sub>7/2</sub> is at 70.5 eV. Details related to the photocatalytic reactor (Figure 1 E) and the measurement of reaction products are given in Supporting Information.

Anodization of pure titanium provides an effective and facile way to generate TiO<sub>2</sub> nanotube arrays with high surface area and controllable dimensions, leading to wide-ranging applications that include solar cells, photocatalysts, and supercapacitors.<sup>[7]</sup> In many cases, however, the photoactivity of TiO<sub>2</sub> nanotubes is limited because of their exclusive absorption of the ultraviolet range of the solar spectrum. The sensitivity of Cu-coated TiO<sub>2</sub> to visible light is partly explained by the interfacial charge-transfer (IFCT) mechanism.<sup>[8]</sup> TiO<sub>2</sub> nanotube arrays with periodically modulated diameters and coaxial bimetallic coatings also function as defect-doped one-dimensional photonic crystals<sup>[9]</sup> that trap light and improve its utilization in photocatalysis. The fabrication of such PMTiNTs was enabled by the application

[\*] Dr. X. Zhang, B. Shi, S. Farsinezhad, Prof. K. Shankar  
Department of Electrical and Computer Engineering  
University of Alberta, Edmonton, AB T6G 2V4 (Canada)  
E-mail: kshankar@ualberta.ca

Dr. X. Zhang, F. Han, Prof. G. P. Dechaine  
Department of Chemical and Materials Engineering, University of  
Alberta, Edmonton, AB T6G 2V4 (Canada)

[\*\*] All authors thank NSERC for funding support. Infrastructure used in the project was made possible by a Leaders Opportunity Fund grant to K.S. from the Canada Foundation for Innovation (CFI) and matched by a similar grant from the Alberta Small Equipment Grants Program (SEGP). S.F. thanks Alberta Innovates Technology Futures for scholarship support. K.S. was also supported by a Petro-Canada Young Innovator Award. X.Z. acknowledges Dr. Dimitre Karpuzov and Shihong Xu at the Alberta Centre for Surface Engineering and Science (ACES). S.F. thanks Diane Caird at the X-ray Diffraction Laboratory.

Supporting information for this article is available on the WWW under <http://dx.doi.org/10.1002/anie.201205619>.

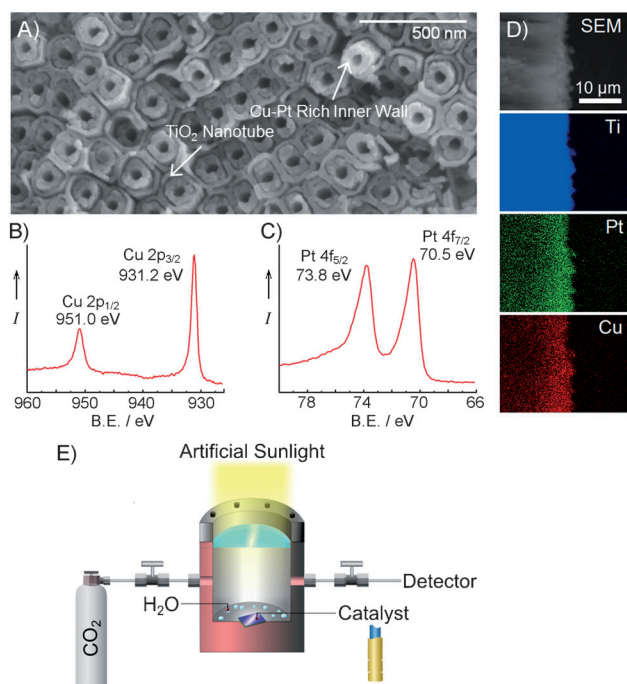


**Figure 1.** A) SEM image taken several  $\mu\text{m}$  deep from the top of a 15  $\mu\text{m}$ -thick PMTiNT-supported Cu-Pt nanocatalyst for solar-driven  $\text{CO}_2$  reduction. A Cu-Pt coated inner wall and a PMTiNT are indicated. B) Cu 2p and C) Pt 4f XPS spectra taken on a Cu-Pt/PMTiNT nanocatalyst. D) Cross-sectional SEM and EDX mapping of Cu-Pt-loaded PMTiNTs. E) Illustration of solar-driven conversion of  $\text{CO}_2$  at room temperature (25  $^\circ\text{C}$ ) using a high-pressure reaction chamber connected directly to a gas chromatograph sampling loop for compositional analysis.

of a sequence of current pulses generated by a switching operation between different individual power supplies during the anodization of titanium (Figure 2 and the Supporting Information, Figure S1).<sup>[9]</sup> PMTiNTs with three repeating segments (200 nm, 60 nm, and 60 nm in length) were fabricated. Note that in galvanostatic pulse anodization, the length of anodized segments was determined by both pulse duration and current magnitude. These freshly formed amorphous  $\text{TiO}_2$  nanotubes, which were subsequently annealed to anatase at 505  $^\circ\text{C}$ , exhibit high photoactivity.

Along with the development of PMTiNTs, a broad range of Cu-Pt compositions of nanotube structures deposited on the calcined  $\text{TiO}_2$  nanotube supports were explored. Core-shell nanotubes with bimetallic coatings on the double-walled  $\text{TiO}_2$  nanotubes were formed by selective photodeposition of Cu-Pt on the inner walls of anatase nanotube arrays in a precursor solution consisting of  $\text{Cu}^{2+}$ ,  $\text{Pt}^{2+}$ , and methanol with different ratios.  $\text{TiO}_2$  nanotube arrays grow with a double-walled structure (Figure 1 A and 2B), which manifests itself during rapid thermal annealing but can also be fused by slow heating to temperatures  $> 550^\circ\text{C}$  to show single walls.<sup>[10]</sup> When processing conditions corresponding to single-walled structures were used, double walls were still observed, suggesting that the conditions of fabricating PMTiNTs generated the double-walled structures in our case (Supporting Information, Figures S2, S3).

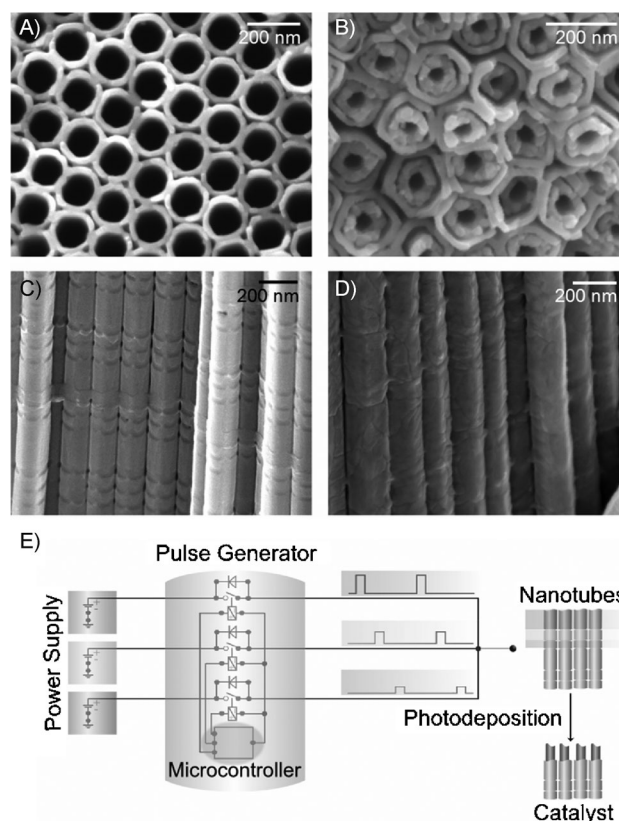


**Figure 2.** A, B) Plan-view and C, D) cross-sectional SEM images of the as-prepared PMTiNT platform (A, C) and Cu-Pt loaded nanotubes (B, D). E) Illustration of the pulse generator employed for the fabrication of PMTiNTs with three repeating segments of 200 nm, 60 nm, and 60 nm in length.

The ability of bimetallic alloys to improve catalytic activity and selectivity has resulted in their use as electrocatalysts in fuel cells and as catalysts in a variety of organic syntheses.<sup>[11]</sup> The combination of noble-metal bimetallic alloys with ordered  $\text{TiO}_2$  nanotube arrays of tunable diameter and wall thickness in core-shell structures offers new possibilities in controlling the shape, size, and composition of the photocatalysts. To investigate the role of Cu-Pt bimetallic coatings in the photocatalytic system, a series of Cu-Pt/ $\text{TiO}_2$  nanocatalysts were prepared and compared to pure copper and platinum-loaded  $\text{TiO}_2$  reference samples in the reduction of  $\text{CO}_2$ . A large number of individual catalysts in which the ratio of Cu/Pt was gradually changed from 1:6 to 5:1 were tested, and the averaged catalytic activity was quantified by the total yield of hydrocarbons (in either molar or volumetric units) per unit catalyst (mass of catalyst or surface area of catalyst wafer) per unit time. Figure 3 A shows a plot of the rate of production of hydrocarbons as a function of Cu/Pt composition in Cu-Pt/ $\text{TiO}_2$  nanocatalysts for a one-hour photoreduction reaction using 0.998 %  $\text{CO}_2$ , wherein the overall hydrocarbon production rate was maximized (3.73  $\text{mL g}^{-1} \text{h}^{-1}$ ) when  $\text{Cu}_{0.33}\text{-Pt}_{0.67}/\text{TiO}_2$  was employed. In this plot, one distinguishable region was observed in the range from Cu-50 % to Cu-85 %, which exhibits a minimum hydrocarbon production rate at Cu-75 %. The rate of  $\text{CH}_4$  produced

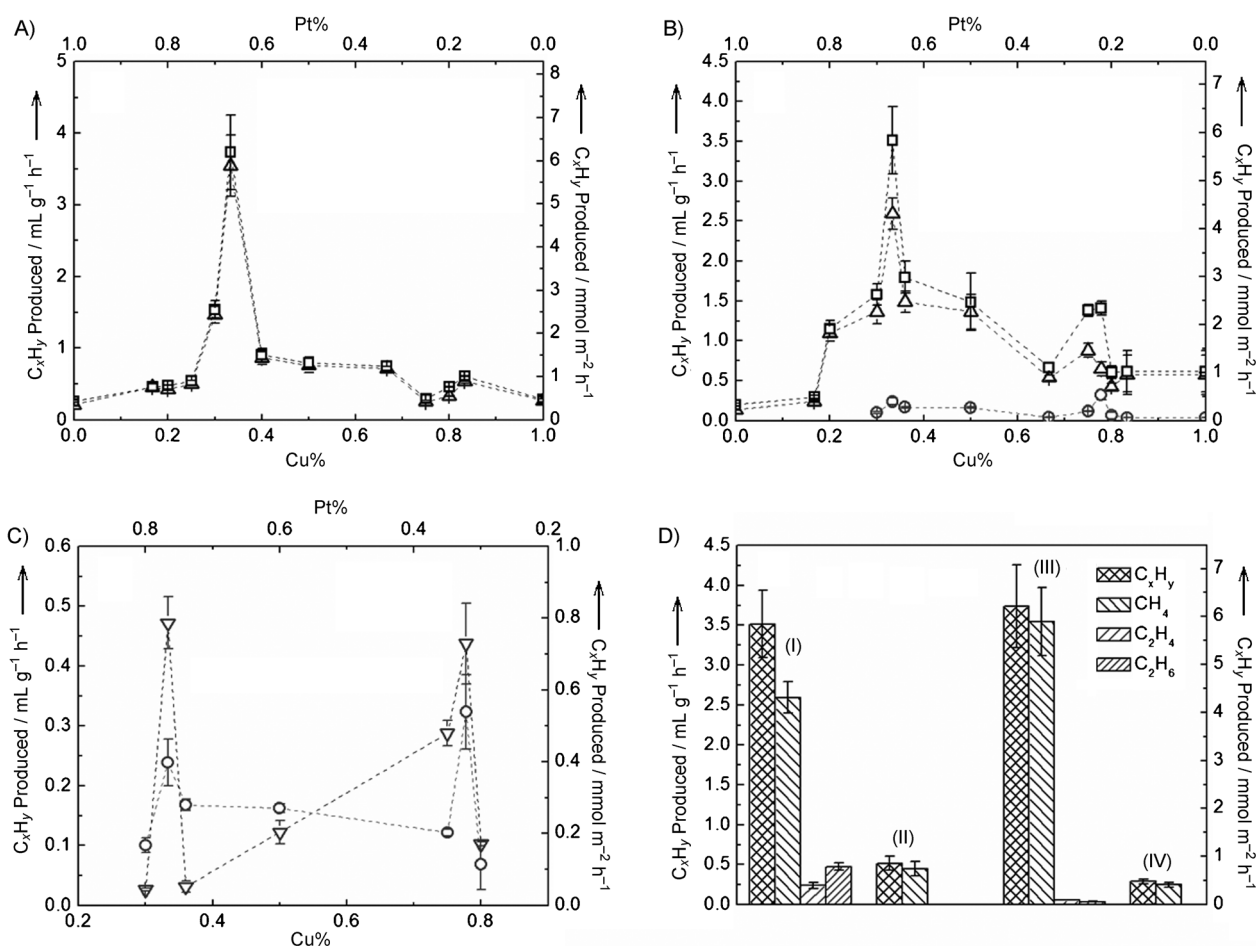


**Figure 3.** A, B) Plots of hydrocarbon (□), CH<sub>4</sub> (△), and C<sub>2</sub>H<sub>4</sub> (○) solar-driven generation rates against fraction of Cu in Cu-Pt bimetallic system using 0.998% (A) and 99.9% (B) CO<sub>2</sub>. C) Comparison of the C<sub>2</sub>H<sub>4</sub> (○) and C<sub>2</sub>H<sub>6</sub> (▽) solar-driven generation rates against fraction of Cu in the Cu-Pt bimetallic system using 99.9% CO<sub>2</sub>. D) Comparison of hydrocarbon generation activities of Cu<sub>0.33</sub>-Pt<sub>0.67</sub> nanotube-loaded PMTiNTs (I, III) and regular TiNTs (II, IV) using 99.9% (I, II) and 0.998% (III, IV) CO<sub>2</sub>.

during the one-hour reduction of 0.998% CO<sub>2</sub> reached a maximum at Cu<sub>0.33</sub>-Pt<sub>0.67</sub> (3.55 mL g<sup>-1</sup> h<sup>-1</sup>), whereas Cu<sub>0.75</sub>Pt<sub>0.25</sub> gave the lowest CH<sub>4</sub> production rate (0.26 mL g<sup>-1</sup> h<sup>-1</sup>). The hydrocarbon production trends are qualitatively the same when using 99.9% CO<sub>2</sub>, with the exception of a local peak observed close to Cu-75% (Figure 3B). The maximum production rates of hydrocarbons and CH<sub>4</sub> were also obtained for the higher purity CO<sub>2</sub> with Cu<sub>0.33</sub>-Pt<sub>0.67</sub> (3.51 mL g<sup>-1</sup> h<sup>-1</sup> and 2.60 mL g<sup>-1</sup> h<sup>-1</sup>, respectively), which confirms that the Cu<sub>0.33</sub>-Pt<sub>0.67</sub> was the most reactive catalyst in the Cu-Pt/TiO<sub>2</sub> series for the photocatalytic reduction of CO<sub>2</sub>. More importantly, considerable amounts of C<sub>2</sub>H<sub>4</sub> and C<sub>2</sub>H<sub>6</sub> were produced when 99.9% CO<sub>2</sub> was used, with the production rates of C<sub>2</sub>H<sub>4</sub> (0.33 mL g<sup>-1</sup> h<sup>-1</sup>) and C<sub>2</sub>H<sub>6</sub> (0.47 mL g<sup>-1</sup> h<sup>-1</sup>) maximized at Cu-75% and Cu-33%, respectively (Figure 3B,C). For comparison, even at Cu-33%, there was only 0.06 mL g<sup>-1</sup> h<sup>-1</sup> C<sub>2</sub>H<sub>4</sub> and 0.04 mL g<sup>-1</sup> h<sup>-1</sup> C<sub>2</sub>H<sub>6</sub> produced when reducing 0.998% CO<sub>2</sub>. Overall, the Pt-Cu/TiO<sub>2</sub> catalysts exhibited high catalytic activity for the photo-reduction of CO<sub>2</sub> and gave rise to significant hydrocarbon production at specific Cu-Pt compositions. In contrast, pure copper and pure platinum-loaded periodically modulated nanotube catalysts led to relatively low hydrocarbon produc-

tion rates (0.28 and 0.26 mL g<sup>-1</sup> h<sup>-1</sup> using 0.998% CO<sub>2</sub>, 0.61 and 0.20 mL g<sup>-1</sup> h<sup>-1</sup> using 99.9% CO<sub>2</sub>, respectively). A series of experiments were also performed using regular, smooth-sided TiO<sub>2</sub> nanotube arrays loaded with Cu<sub>0.33</sub>-Pt<sub>0.67</sub> with the same dimensions of the periodically modulated nanotubes to distinguish the effect of such nanostructures on the catalysts. Figure 3D obviously shows that by using these reference samples, the production rate of hydrocarbons dropped 92% and 86% in 0.998% CO<sub>2</sub> and 99.9% CO<sub>2</sub>, respectively, whereas the production rate of CH<sub>4</sub> decreased by 93% and 83%, respectively. In the case of Cu<sub>0.33</sub>-Pt<sub>0.67</sub>-loaded regular TiO<sub>2</sub> nanotubes, no C<sub>2</sub>H<sub>4</sub> or C<sub>2</sub>H<sub>6</sub> products were observed.

In summary, the results reported herein highlight the exploration of easily prepared periodically modulated TiO<sub>2</sub> nanotubes with remarkable photoactivity. Relatively high CO<sub>2</sub>-to-hydrocarbon conversion rates were achieved by coupling bimetallic coatings with these TiO<sub>2</sub> nanotube arrays as catalysts in the photoreduction of CO<sub>2</sub> and H<sub>2</sub>O to hydrocarbons at room temperature. Direct control over TiO<sub>2</sub> nanotube structures using programmed pulse anodization has opened a feasible route to enhance their photocatalytic efficiency, which also benefited the development of the reported catalyst. By varying the fraction of one component



in this bimetallic system, Cu<sub>0.33</sub>-Pt<sub>0.67</sub> has been found to be the most reactive catalyst in its family to generate light hydrocarbons at room temperature using low-concentration CO<sub>2</sub>.

## Experimental Section

**Catalyst Preparation:** Grade 2 pure titanium substrates were degreased in an ultrasonic bath of reagent-grade ethanol for 10 min and tried with nitrogen gas. Electropolishing of titanium was preformed at 0°C in perchloric acid (0.100M in glacial acetic acid, Ricca Chemical) for 10 min using constant voltage (125 V). The substrates were then removed from the polishing solution, cleaned ultrasonically with isopropyl alcohol for 5 min, and dried with a nitrogen gas flow.

Periodically modulated titania nanotube (PMTiNT) platforms were synthesized by pulse anodization of pre-electropolished titanium substrates in a two-electrode anodization setup using a graphite counter electrode. Before anodization, these titanium substrates were cleaned ultrasonically with acetone and isopropyl alcohol, and then dried by a stream of nitrogen gas. Pulse anodization of titanium that has been discussed in the paper was carried out at 15°C in an EG electrolyte, which consists of a mixture of NH<sub>4</sub>F (0.25%, w/w), deionized water (3%, v/v), and ethylene glycol. Constant applied currents were used during the anodization. After anodization, the substrates were removed from the electrolyte solution, rinsed with isopropyl alcohol, and dried with nitrogen gas. The annealing of as-prepared PMTiNTs was carried out at 505°C for 8 h with a ramping rate of 1.3°Cmin<sup>-1</sup> in a 3-zone tube furnace (Lindberg/Blue M, Thermo Scientific).

A growth solution was prepared by mixing K[PtCl<sub>4</sub>] (0.5–2 mM, aq)/[Pt(acac)<sub>3</sub>] (0.5–2 mM, in methanol), [Cu(acac)<sub>3</sub>] (0.5–2 mM, in methanol), methanol, and deionized water at room temperature using ultrasonication. A teflon reaction cell was designed and constructed to match the dimension of the sample. To prepare the catalysts, annealed PMTiNT platforms were soaked in the growth solution and the photodeposition of metallic nanotubes was carried out for 45–60 min under the irradiation of a 4 W 365 nm screen-inspection UV lamp (1000 μWcm<sup>-2</sup>). The PMTiNT platforms were then removed from the growth solution and rinsed thoroughly with isopropyl alcohol, dried by nitrogen gas.

Samples were characterized by scanning electron microscopy (SEM) and X-ray photoelectron spectroscopy (XPS). The SEM images were taken with a Hitachi S-4800FE-SEM. XPS measurements were carried out under UHV conditions (<10<sup>-8</sup> Torr) on a Kratos Analytical, Axis-Ultra instrument. Wide angle X-ray diffraction data (Supporting Information, Figure S4) were collected using a Rigaku Ultima IV diffractometer.

The photoreduction of CO<sub>2</sub> was carried out at room temperature in a dark room. A Newport solar simulator (91160–1000) equipped with Class A filters was employed as the light source. The distance between the catalyst surface and the lens of the solar simulator is 32 cm. AM1.5 sunlight was used for all experiments. Catalyst film area: circa 1.8 cm<sup>2</sup>; mass of the catalyst film (Cu-Pt + TiO<sub>2</sub>): circa 6.7 mg. To measure the mass of the catalyst, the Cu-Pt-coated PMTiNT thin films were detached from the titanium substrate using mechanical forces and carefully weighed.

Gas chromatography determinations were carried out by a Varian Star (Varian, CA, USA) equipped with a Porapak QS column (12 Ft; 366 cm; 3.2 mm OD, 2 mm ID). A TCD detector and a FID detector were employed. The detector temperature was held at 180°C and 250°C for TCD and FID, respectively. The column temperature was held at 70°C. Helium was used as the carrier gas.

Received: July 15, 2012

Revised: September 30, 2012

Published online: November 9, 2012

**Keywords:** bimetallic alloys · core-shell particles · photodeposition · photonic crystals · semiconductor photocatalysis

- [1] N. S. Lewis, D. G. Nocera, *Proc. Natl. Acad. Sci.* **2006**, *103*, 15729.
- [2] S. J. Davis, K. Caldeira, H. D. Matthews, *Science* **2010**, *329*, 1330.
- [3] T. Inoue, A. Fujishima, S. Konishi, K. Honda, *Nature* **1979**, *277*, 637.
- [4] a) W. C. Chueh, C. Falter, M. Abbott, D. Scipio, P. Furler, S. M. Haile, A. Steinfeld, *Science* **2010**, *330*, 1797; b) T. Yui, A. Kan, C. Saitoh, K. Koike, T. Ibusuki, O. Ishitani, *ACS Appl. Mater. Interf.* **2011**, *3*, 2594; c) N. M. Dimitrijevic, B. K. Vijayan, O. G. Poluektov, T. Rajh, K. A. Gray, H. Y. He, P. Zapol, *J. Am. Chem. Soc.* **2011**, *133*, 3964; d) Y. Y. Liu, B. B. Huang, Y. Dai, X. Y. Zhang, X. Y. Qin, M. H. Jiang, M. H. Wangbo, *Catal. Commun.* **2009**, *11*, 210.
- [5] a) X. Chen, S. S. Mao, *Chem. Rev.* **2007**, *107*, 2891; b) X. B. Chen, L. Liu, P. Y. Yu, S. S. Mao, *Science* **2011**, *331*, 746; c) D. Wang, L. Liu, F. Zhang, K. Tao, E. Pippel, K. Domen, *Nano Lett.* **2011**, *11*, 3649.
- [6] a) O. K. Varghese, M. Paulose, T. J. LaTempa, C. A. Grimes, *Nano Lett.* **2009**, *9*, 731; b) W.-N. Wang, W.-J. An, B. Ramalingam, S. Mukherjee, D. M. Niedzwiedzki, S. Gangopadhyay, P. Biswas, *J. Am. Chem. Soc.* **2012**, *134*, 112760; c) C. Wang, R. L. Thompson, J. Baltrus, C. Matrangola, *J. Phys. Chem. Lett.* **2010**, *1*, 48; d) C. Wang, R. L. Thompson, P. Ohodnicki, J. Baltrus, C. Matrangola, *J. Mater. Chem.* **2011**, *21*, 13452.
- [7] a) F. Fábregat-Santiago, E. M. Barea, J. Bisquert, G. K. Mor, K. Shankar, C. A. Grimes, *J. Am. Chem. Soc.* **2008**, *130*, 11312; b) O. K. Varghese, M. Paulose, C. A. Grimes, *Nat. Nano* **2009**, *4*, 592; c) K. Shankar, J. I. Basham, N. K. Allam, O. K. Varghese, G. K. Mor, X. Feng, M. Paulose, J. A. Seabold, K.-S. Choi, C. A. Grimes, *J. Phys. Chem. C* **2009**, *113*, 6327; d) W. X. Guo, X. Y. Xue, S. H. Wang, C. J. Lin, Z. L. Wang, *Nano Lett.* **2012**, *12*, 2520.
- [8] a) H. Irie, K. Kamiya, T. Shibamura, S. Miura, D. A. Tryk, T. Yokoyama, K. Hashimoto, *J. Phys. Chem. C* **2009**, *113*, 10761; b) H. Irie, S. Miura, K. Kamiya, K. Hashimoto, *Chem. Phys. Lett.* **2008**, *457*, 202; c) K. Kamiya, S. Miura, K. Hashimoto, H. Irie, *Electrochemistry* **2011**, *79*, 793; d) M. Liu, X. Q. Qiu, M. Miyauchi, K. Hashimoto, *Chem. Mater.* **2011**, *23*, 5282; e) A. Nakajima, Y. Akiyama, S. Yanagida, T. Koike, T. Isobe, Y. Kameshima, K. Okada, *Mater. Lett.* **2009**, *63*, 1699.
- [9] a) W. Chanmanee, A. Watcharenwong, C. R. Chenthamarakshan, P. Kajitvichyanukul, N. R. de Tacconi, K. Rajeshwar, *J. Am. Chem. Soc.* **2008**, *130*, 965; b) C. T. Yip, H. T. Huang, L. M. Zhou, K. Y. Xie, Y. Wang, T. H. Feng, J. S. Li, W. Y. Tam, *Adv. Mater.* **2011**, *23*, 5624.
- [10] a) Q. A. S. Nguyen, Y. V. Bhargava, V. R. Radmilovic, T. M. Devine, *Electrochim. Acta* **2009**, *54*, 4340; b) S. P. Albu, A. Ghicov, S. Aldabergenova, P. Drechsel, D. LeClere, G. E. Thompson, J. M. Macak, P. Schmuki, *Adv. Mater.* **2008**, *20*, 4135.
- [11] a) B. Lim, M. J. Jiang, P. H. C. Camargo, E. C. Cho, J. Tao, X. M. Lu, Y. M. Zhu, Y. N. Xia, *Science* **2009**, *324*, 1302; b) D. C. Powers, T. Ritter, *Nat. Chem.* **2009**, *1*, 302; c) V. R. Stamenkovic, B. S. Mun, M. Arenz, K. J. J. Mayrhofer, C. A. Lucas, G. F. Wang, P. N. Ross, N. M. Markovic, *Nat. Mater.* **2007**, *6*, 241; d) F. Tao, M. E. Grass, Y. W. Zhang, D. R. Butcher, J. R. Renzas, Z. Liu, J. Y. Chung, B. S. Mun, M. Salmeron, G. A. Somorjai, *Science* **2008**, *322*, 932.